Supporting Information

Stavropoulos *et al.* 10.1073/pnas.0805813105

SI Text

Plasmid Constructs. A DNA fragment comprising of full-length *S. cerevisiae* Rtt109 (residues 1–436) was amplified by PCR from genomic DNA. The full-length Rtt109 was used as a PCR template to generate the Rtt109ΔL variant, in which a four-residue linker of sequence GGSG replaced residues 128–170. For protein expression in *E. coli*, Rtt109 fragments were cloned into a modified pET28a vector (Novagen) that contained an N-terminal hexahistidine tagged SUMO. Rtt109 mutants were generated by QuikChange mutagenesis (Stratagene) and confirmed by DNA sequencing. For yeast experiments, various Rtt109 variants were subcloned into the expression vector pRS416 (ATCC). A DNA fragment containing the full-length *S. cerevisiae* Vps75 (residues 1–264) was amplified by PCR using genomic DNA and subsequently cloned into a modified pET28a vector that contained an N-terminal hexahistidine tag, followed by a PreScission protease cleavage site (1). A DNA fragment of *S. cerevisiae* ASF1, containing residues 1–169 was amplified by PCR using genomic DNA and cloned into a modified pET28a vector that contains an N-terminal GST tag followed by a PreScission protease cleavage site.

Protein Expression and Purification. Rtt109 was expressed in *E. Coli* BL21-CodonPlus(DE3)-RIL cells (Stratagene). Protein expression was induced with 500 μM isopropyl-β-D-thiogalactoside (IPTG) at 27°C for 5 h in LB media. Cells were harvested by centrifugation and resuspended in a buffer containing 20 mM Tris, pH 7.6, 300 mM NaCl, 5% (vol/vol) glycerol, 20 mM 2-mercaptoethanol, 10 mM imidazole, and Complete EDTA-free protease inhibitor mixture tablets (Roche). The cells were lysed with a cell disrupter (Avestin), and the lysate was centrifuged for 90 min at 40,000 $\times$ *g*. The lysate was then applied onto a Ni-NTA column (Qiagen) and eluted via an imidazole gradient. Fractions containing Rtt109 proteins were pooled, dialyzed against a buffer containing 20 mM Tris (pH 7.6), 300 mM NaCl, 5% (vol/vol) glycerol, and 20 mM 2-mercaptoethanol, cleaved with the SUMO specific protease Ulp1 for 12 h, and rerun over a Ni-NTA column to remove hexahistidine-tagged SUMO. Fractions testing positive for Rtt109 proteins were applied to a HiTrap Heparin column and eluted via a NaCl gradient (300–800 mM). Rtt109 proteins' positive fractions were pooled and further purified by using a 16/60 Superdex 200 column (GE Healthcare) equilibrated in 20 mM Tris (pH 7.6), 300 mM NaCl, 5% (vol/vol) glycerol, and 5 mM DTT. Fractions containing Rtt109 proteins were pooled and concentrated for crystallization. Vps75 and Asf1 were expressed and purified as Rtt109 with the exception of cleavage of the hexahistidine tag being conducted using PreScission protease (GE Healthcare). Asf1 was expressed and purified as Rtt109 with the exception of the affinity chromatography steps being carried out on a GST-Sepharose column (GE Healthcare).

Crystallization and Structure Determination. Crystals of Rtt109ΔL were grown at 21°C in hanging drops containing 1 μl of the protein (25 mg/ml), which contained a twofold molar excess of acetyl CoA and 1 μl of a reservoir solution consisting of 12–15% (wt/vol) PEG 4,000, 1 mM $ZnCl_2$, and 100 mM sodium acetate (pH 4.3–4.6). Initial crystals grew as small clusters. The shape and size of these crystals were substantially improved by micro seeding techniques. Single crystals of Rtt109ΔL were grown at 21°C in hanging drops containing 1 μl of a diluted seed stock, 2 μl of the protein (2–5 mg/ml) containing a twofold molar excess of acetyl CoA, and 2 μl of a reservoir solution consisting of 2–8% (wt/vol) PEG 4,000, 1 mM $ZnCl_2$, and 100 mM sodium acetate (pH 4.3–4.6). Crystals grew in the monoclinic space group C2, with one molecule in the asymmetric unit, and they grew to their maximum size 200 μm $\times$ 150 μm $\times$ 50 μm within 10 days. For cryoprotection, crystals were stabilized in 15% (wt/vol) PEG 4,000, 1 mM $ZnCl_2$, 100 mM sodium acetate (pH 4.6), and 20% (vol/vol) glycerol and flash-frozen in liquid nitrogen-cooled liquid propane. X-ray diffraction data were collected at the National Synchrotron Light Source (NSLS), Brookhaven National Laboratory (BNL), beamline X3A (Table S1). X-ray intensities were processed by using the HKL2000 denzo/scalepack package (2), and the CCP4 program package (3) was used for subsequent calculations.

A single-wavelength anomalous dispersion (SAD) x-ray diffraction dataset of a seleno-L-methionine (SeMet)-labeled protein crystal was used to identify the positions of five selenium atoms by using SHELXD (4). Phases were calculated to 2.0Å in SHARP (5), followed by density modification in DM (CCP4) with solvent flattening and histogram matching. This procedure yielded an electron density map of high quality. A model lacking only the C-terminal 35 residues was built with the program O (6). The model was refined by using CNS (7) and Refmac (3) using the TLS option, and the stereochemical quality of the model was assessed with PROCHECK (8). There are no residues in the disallowed region of the Ramachandran plot.

DNA Damage Hypersensitivity Assay. Rtt109 constructs were transformed into BY4741 wild-type and BY4741 *rtt109*Δ::*kan* strains (Open Biosystems), by using standard LiCl transformation protocols, and plated on SD-URA plates. Liquid cultures of the transformants were grown overnight at 30°C in SD-URA media. Cells were counted and diluted to 250,000 cells per ml. This stock was used to generate a tenfold dilution series of which 10 μl were spotted on SD-URA plates, containing camptothecin (CPT, 1–5 μg/ml), hydroxyurea (HU, 3.8–11.4 mg/ml), or methyl methanesulfonate (MMS, 13–130 μg/ml), and grown at 30°C for 2–3 days.

Protein Interaction Analysis. Protein interaction experiments were carried out on a Superdex 200 10/300 GL gel filtration column (GE Healthcare) in a buffer containing 20 mM Tris (pH 7.6), 300 mM NaCl, 5% (vol/vol) glycerol, and 5 mM DTT. To assess complex formation, 750 μg of purified Rtt109, Rtt109ΔL, or Vps75 were either injected individually or injected after mixing and incubating for 30 min on ice. All final sample volumes were 150 μl.

Illustrations and Figures. Figures were generated by using PyMOL (www.pymol.org). The molecular surfaces were calculated by using MSMS (9), and the electrostatic potential was calculated by using APBS (10). Sequence alignments were generated by using ClustalX (11) and colored with Alscript (12).

1. Hoelz A, Nairn AC, Kuriyan J (2003) Crystal structure of a tetradecameric assembly of the association domain of Ca2+/calmodulin-dependent kinase II. *Mol Cell* 11:1241–1251.
2. Otwinowski Z, Minor W (1997) Processing of x-ray diffraction data collected in oscillation mode. *Methods Enzymol* 276:307–326.
3. CCP4 (1994) Collaborative Computational Project, Number 4, The CCP4 Suite: Programs for Protein Crystallography. *Acta Crystallogr D* 50:760–763.
4. Schneider TR, Sheldrick GM (2002) Substructure solution with SHELXD. *Acta Crystallogr D* 58:1772–1779.

5. La Fortelle ED, Bricogne G (1997) Maximum-likelihood heavy-atom parameter refinement in the MIR and MAD methods. *Methods Enzymol* 276:476–494.
6. Jones TA, Zou JY, Cowan SW, Kjeldgaard M (1991) Improved methods for building protein models in electron density maps and the location of errors in these models. *Acta Crystallogr A* 47:110–119.
7. Brunger AT, *et al.* (1998) Crystallography & NMR system: A new software suite for macromolecular structure determination. *Acta Crystallogr D* 54:905–921.
8. Laskowski RA, MacArthur MW, Moss DS, Thornton JM (1993) PROCHECK: A program to check the stereochemical quality of protein structures. *J Appl Crystallogr* 26:283–291.
9. Sanner MF, Olson AJ, Spehner JC (1996) Reduced surface: An efficient way to compute molecular surfaces. *Biopolymers* 38:305–320.
10. Baker NA, Sept D, Joseph S, Holst MJ, McCammon JA (2001) Electrostatics of nanosystems: Application to microtubules and the ribosome. *Proc Natl Acad Sci USA* 98:10037–10041.
11. Jeanmougin F, Thompson JD, Guoy M, Higgins DG, Gibson TJ (1998) Multiple sequence alignment with Clustal X. *Trends Biochem* 23:403–405.
12. Barton GJ (1993) ALSCRIPT: A tool to format multiple sequence alignments. *Protein Eng* 6:37–40.

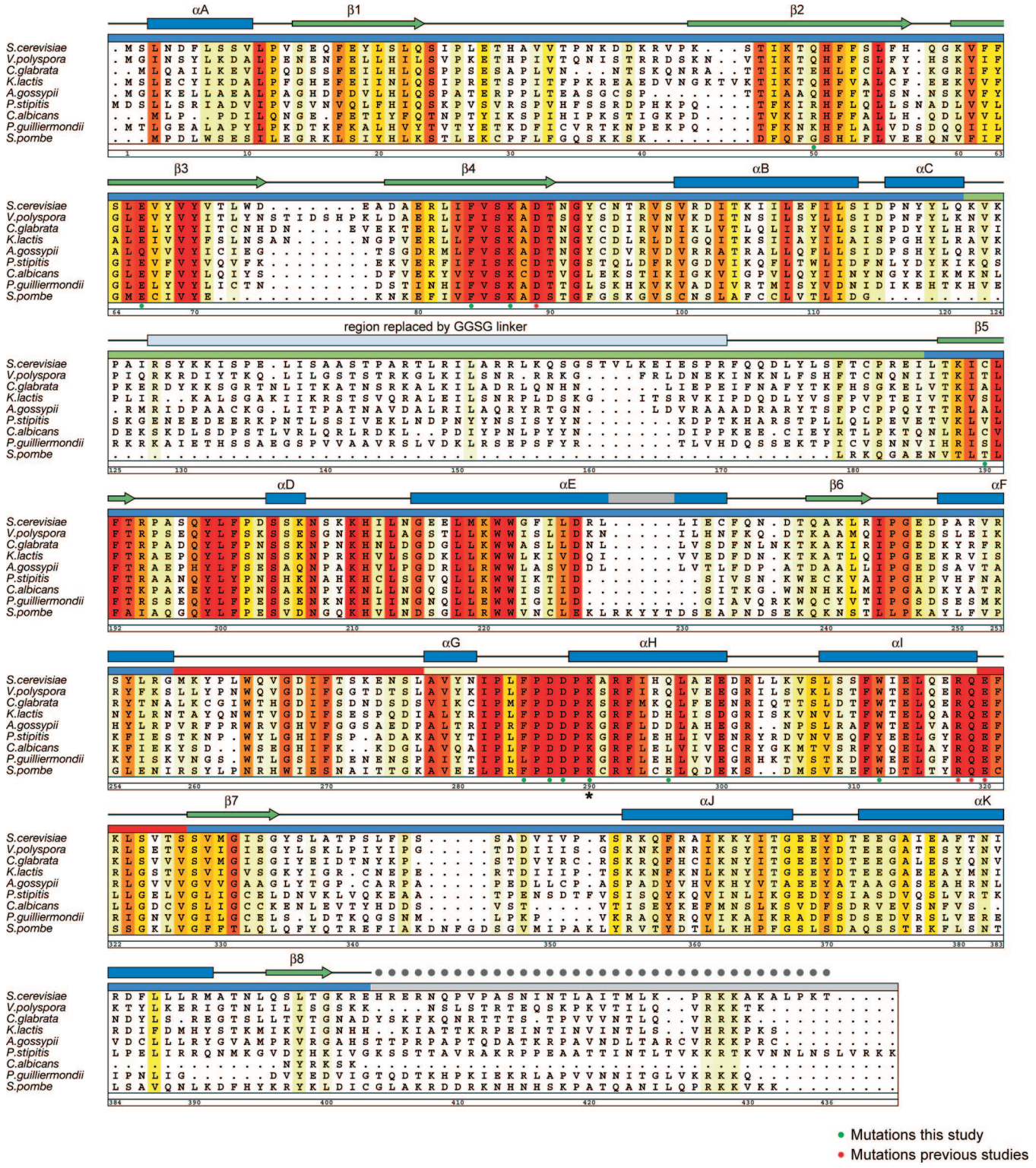

Fig. S1. Multispecies sequence alignment of Rtt109 homologs. The numbering below the alignment is relative to *S. cerevisiae* Rtt109. The overall sequence conservation at each position is shaded in a color gradient from yellow (40% similarity) to dark red (100% identity), by using the Blosum62 weighting algorithm. The secondary structure is indicated above the sequence as green arrows (β-strands), blue rectangles (α-helices), gray lines (coil regions), and gray dots (disordered residues). Residues that are important for enzymatic activity (green dots, this study; red dots, previous studies) and the acetylated K290 (star) are indicated below the aligned sequences.

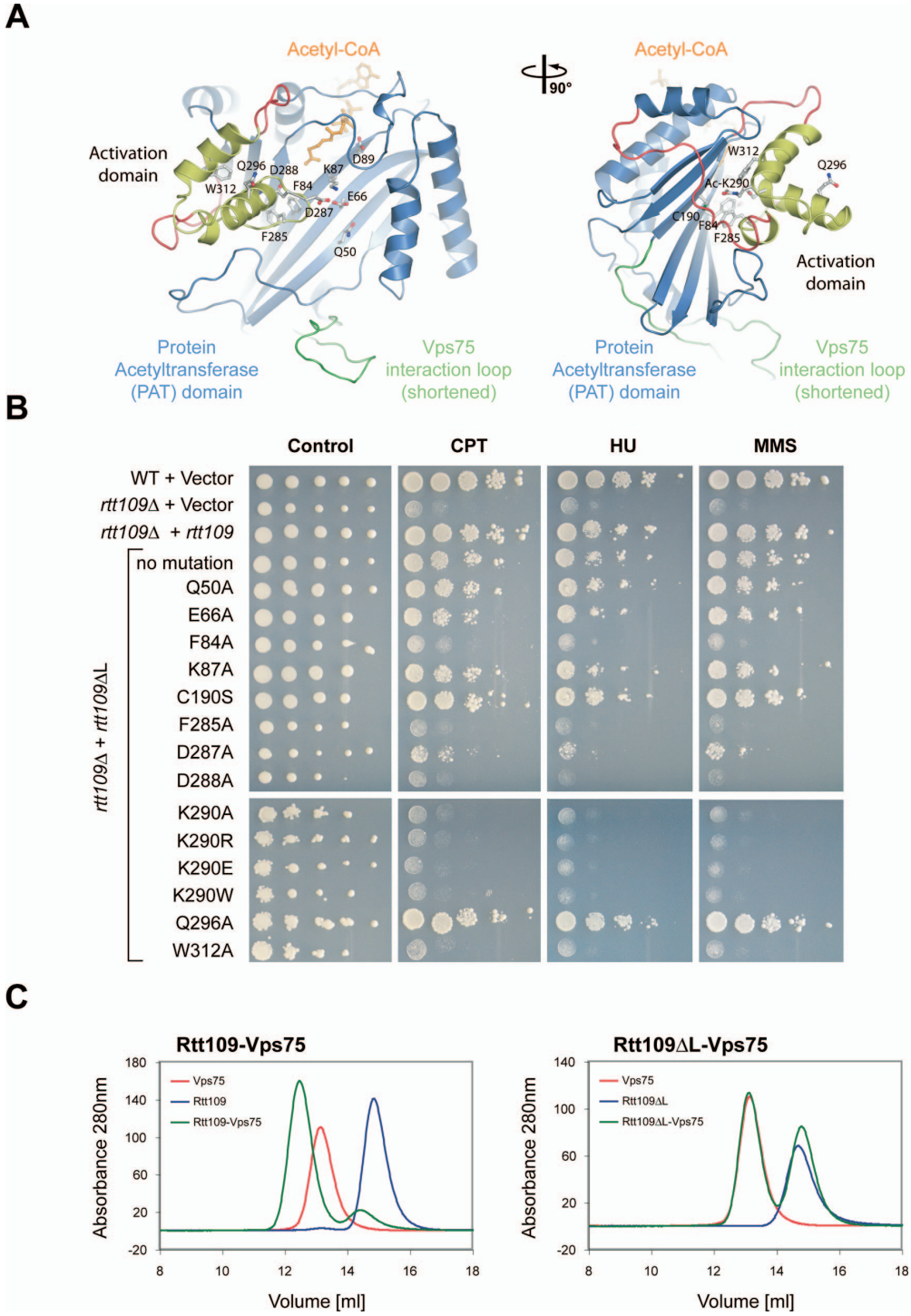

Fig. S2. Mutational analysis of Rtt109. (*A*) Ribbon representation of Rtt109, colored according to Fig. 1*A*. Mutated residues are illustrated in ball-and-stick representation. A 90°-rotated view is shown on the right. (*B*) *In vivo* analysis of Rtt109 mutants in a DNA damage hypersensitivity assay. Serial dilutions (10-fold) of wild-type or rtt109Δ cells transformed with wild-type or the indicated mutants were spotted on SD-URA plates alone or on SD-URA plates containing camptothecin (CPT) at 1 μg/ml, hydroxyurea (HU) at 7.6 mg/ml, or methyl methanesulfonate (MMS) at 65 μg/ml. (*C*) Biochemical analysis of the interaction between Rtt109 and Vps75. Gel filtration profiles of full-length Rtt109, Vps75, and their complex (*Left*) and Rtt109ΔL, Vps75, and their coinjection (*Right*). The Rtt109–Vps75 interaction depends on the Vps75 interaction loop. In the Rtt109ΔL structure, the Vps75 interaction loop is genetically shortened and does not contain the Vps75 interaction region.

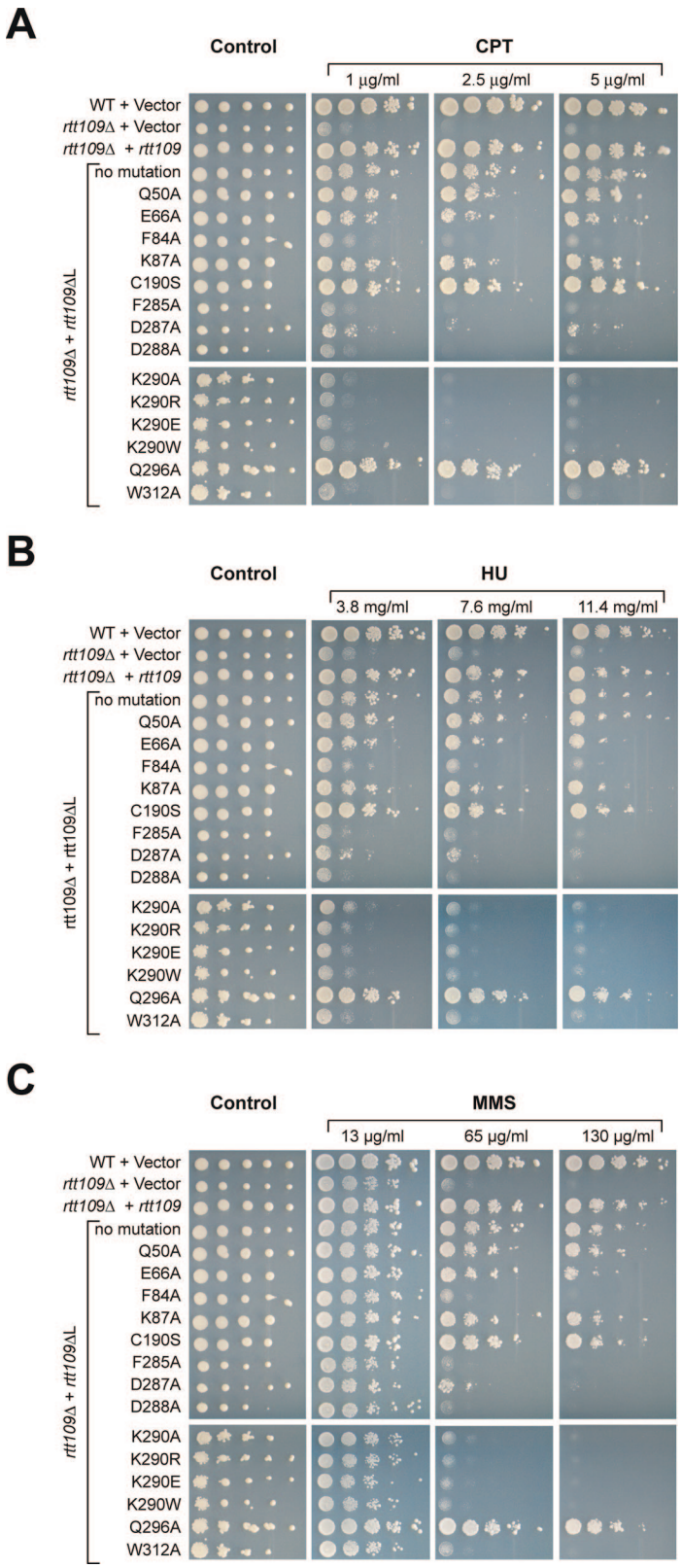

Fig. S3. Mutational analysis of Rtt109 in a DNA damage hypersensitivity assay. Serial dilutions (10-fold) of wild-type or *rtt109*Δ cells transformed with wild type or the indicated mutants were spotted on SD-URA plates alone or on SD-URA plates containing camptothecin (CPT) at a concentration of 1–5 μg/ml (*A*), hydroxyurea (HU) at a concentration of 3.8–11.4 mg/ml (*B*), or methyl methanesulfonate (MMS) at a concentration of 13–130 μg/ml (*C*).

Table S1. Crystallographic analysis

	Crystal 1 SeMet
Data collection	
Synchrotron	BNL-NSLS
Beamline	X3A
Space group	C2
Cell dimensions	
a, *b*, *c*, Å	120.7, 68.9, 55.1
α, β, γ , °	$\alpha = \gamma = 90$, $\beta = 106.7$
	Se Peak
Wavelength, Å	0.97885
Resolution, Å	50.0–2.0
R_{sym}	9.3 (25.0)
$\langle I/\sigma I \rangle$	22.5 (7.9)
Completeness, %	100.0 (100.0)
Redundancy	7.7 (7.3)
Refinement	
Resolution, Å	50.0–2.0
No. of reflections	
Total	55,305
Test set	5,432 (9.4%)
R_{work}/R_{free}	15.6 / 18.6
No. of atoms	3,289
Protein	2,960
Ligand/ion	51
Water	278
B-factors	21
Protein	20
Ligand/ion	21
Water	31
R.m.s deviations	
Bond lengths, Å	0.014
Bond angles, °	1.5

*Highest-resolution shell is shown in parentheses.

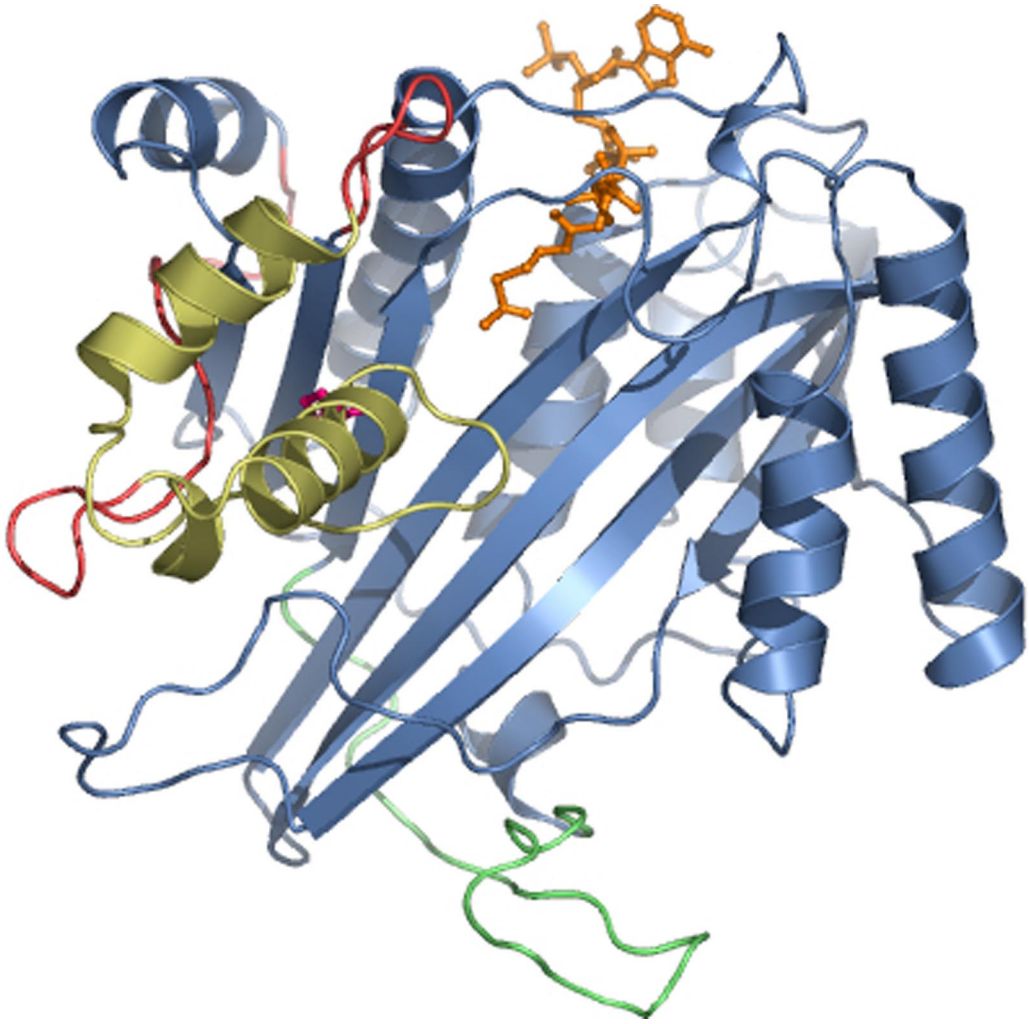

Movie S1. Rotating structure of Rtt109 in ribbon representation.

Movie S1 (MOV)

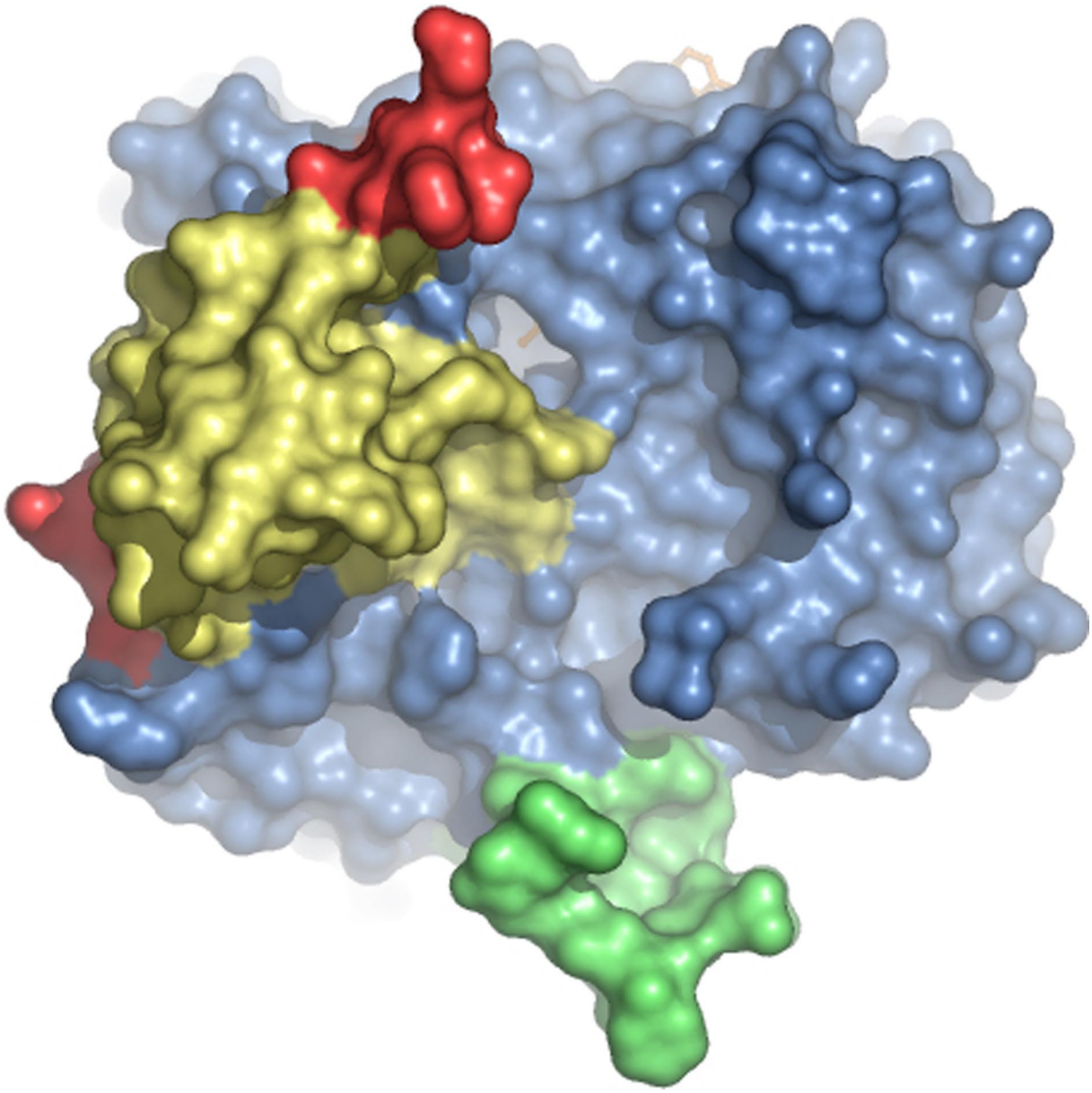

Movie S2. Rotating structure of Rtt109 in surface representation. The acetyl-CoA cofactor is shown in orange ball-and-stick representation.

Movie S2 (MOV)

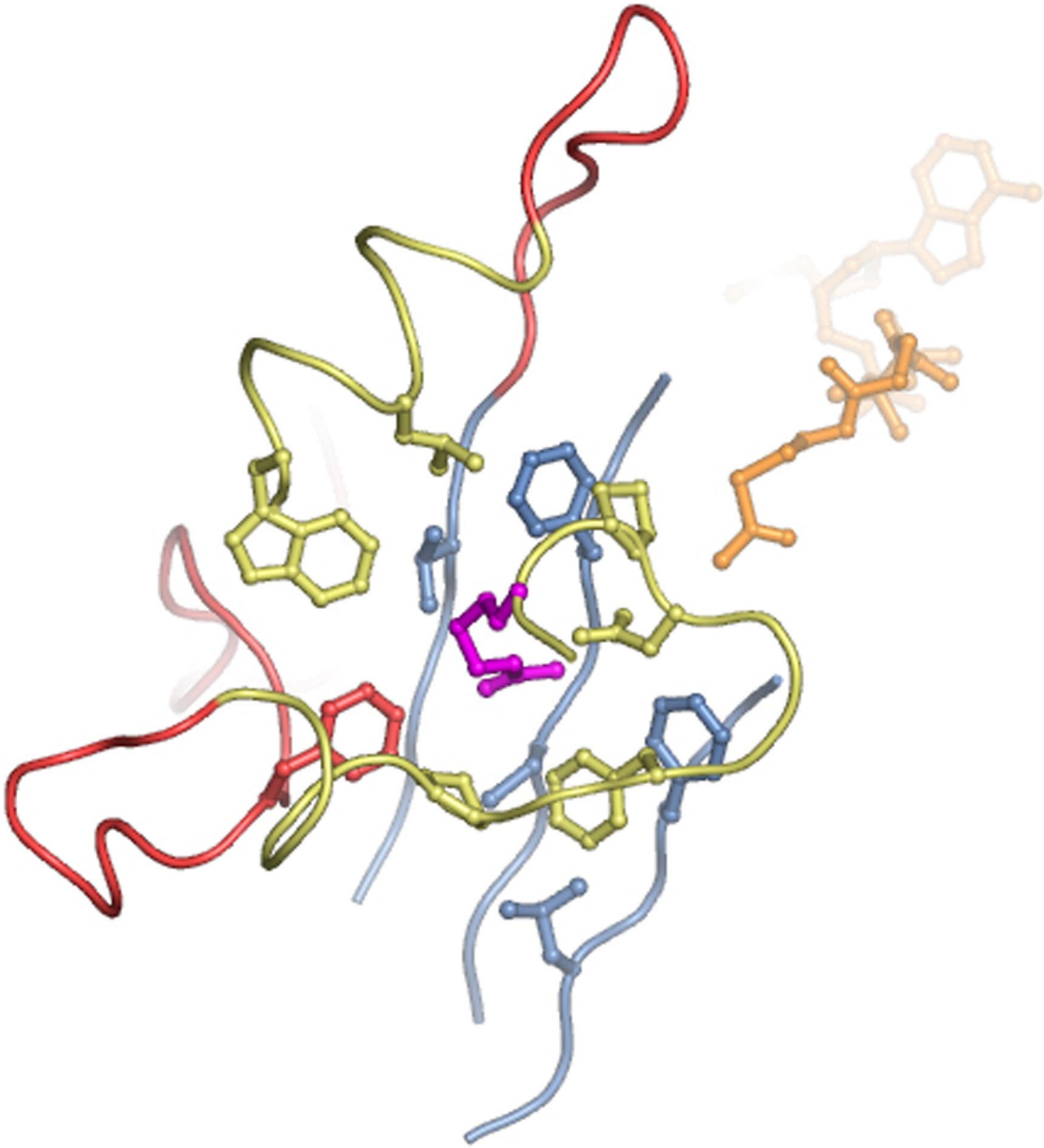

Movie S3. Rotating structure of the hydrophobic cage around the acetylated lysine-290. Residues are colored according to Fig. 1.

Movie S3 (MOV)